Design and Implementation of a High Gain Hexagon Loop Antenna for 5G and WLAN Application

Ali Y. Al-Zahrani
Department of Electrical and Electronic Engineering, College of Engineering, University of Jeddah, Jeddah 21589, Saudi Arabia
ayalzahrani1@uj.edu.sa

Mohd Najim
Department of Electrical and Electronic Engineering, College of Engineering, University of Jeddah, Jeddah 21589, Saudi Arabia
mngalib@uj.edu.sa (corresponding author)

Received: 22 March 2024 | Revised: 11 May 2024 | Accepted: 29 May 2024

 DOI: https://doi.org/10.48084/etasr.7323

ABSTRACT

In this work, the design and implementation of a high-gain Hexagon Loop Antenna (HLA) for 5G and WLAN application is presented. Initially, a hexagon patch was designed to resonate at 3.5 GHz. A loop-based radiator was tailored to obtain miniaturization without affecting the overall performance of the proposed antenna. A CPW feed was utilized to maintain the wide bandwidth with improved return loss. FR-4 material was used as a dielectric to retain the low cost of the antenna. The return loss was kept well below -10 dB, from 3.2 GHz to 6.4 GHz. The gain of the proposed Microstrip Hexagon Loop Antenna (MHLA) is 5.3 dBi at 3.5 GHz and 8.2 dBi at 5.8 GHz, respectively. To improve the gain and directivity of the proposed antenna, a square-shaped AMC unit cell was considered, and finally, a [4×4] ground plane AMC was integrated with the antenna. The radiation pattern of the antenna is stable and low cross-polarization is maintained for the desired band. A simulation of the proposed antenna was carried out in the ANSYS HFSS tool and the experimental results were measured inside an anechoic chamber. The experimental and simulated results of the proposed antenna are in good agreement. Its simple and low-profile structure, lower cost, and high gain ensure that the proposed high gain antenna is well suited for sub-6 GHz band and wireless application.

Keywords-loop antenna; hexagon; high gain; 5G; miniaturization

I. INTRODUCTION

Nowadays, numerous planar antenna designs applicable for several wireless applications, such as wireless, IoT, WLAN, WiMAX, and 5G have emerged. The present research work discloses a high-gain antenna that exhibits a frequency response suitable for 5G, WLAN, and many other wireless applications. A compact structure with low cost and high gain is crucial to maintain the industry demand in the direction of wireless applications [1, 2]. As the most recent generation of wireless technology, 5G applications have recently become a more active area of research. These applications call for a simple low-cost antenna with consistent gain over the appropriate frequency band, which ensures high-speed and reliable connection [3]. Antenna design needs extra care as it is being used for both the receiver and the transmitter ends. Several 5G antennas with a low cost and small area have been reported and presented [4-8], but their structures were bulky and complex to maintain more than 5 dBi gains over the band of interest [9-10]. Authors in [11, 12] have reported the use of a Co-Planar Waveguide (CPW) feed for bandwidth enhancement in planar antenna design. It has been discussed that in order to improve the bandwidth one can reduce the size of the ground plane, rendering the reduction in directivity and gain unavoidable. In [13-17], the authors have reported a gain enhancement technique deploying an Artificial Magnetic Conductor (AMC) as a ground plane without affecting the impedance bandwidth of the proposed antennas. The gain was improved utilizing AMC as the ground plane beneath the antennas, but, on the other hand, the return loss and radiation patterns were compromised [11, 13]. This drawback of high gain antenna design demands an economical solution without affecting the antenna parameters.

This work performed a detailed study of the loop-based antenna to achieve a simple and effective antenna model with improved bandwidth, which operates at 3.5 and 5.8 GHz bands with -10 dB return loss. The achieved bandwidth ranges from

2.5 GHz to 7.0 GHz. The proposed designs have better return loss, wide bandwidth, and provide a stable radiation pattern over the entire band of application. Furthermore, to improve the radiation property and the directivity of the proposed loop antenna, AMC unit cells were designed and integrated to the antenna. Antennas were fabricated and tested inside the anechoic chamber to validate the simulation results.

II. DESIGN OF LOOP ANTENNA

Initially, a Monopole Hexagon Patch Antenna (MHPA) is designed for 3.5 GHz resonance frequency using the standard antenna design equation as presented in [1]. The substrate material utilized to design the antenna is FR-4 with a dielectric constant of 4.4 and tangential loss of 0.002. Recently, it was reported that monopole antennas might be made smaller by employing loop-based structures [2-3]. To achieve wideband response, a hexagon radiating patch was tailored into a Microstrip Hexagon Loop Antenna (MHLA). Return loss was well below -10 dB from 2.5 GHz to 6.0 GHz and the obtained bandwidth was 18% reduced for the desired resonance frequency. Figure 1 portrays the proposed MHLA, while the dimensions are presented in Table I.

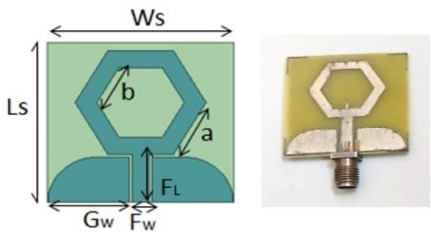

Fig. 1. The proposed MHLA.

TABLE I. DESIGN PARAMETERS OF THE PROPOSED ANTENNA

Parameters	Values (mm)	Parameters	Values (mm)
(Ls) Substrate length	30	(F_L) Feed length	13
(Ws) Substrate width	30	(Fw) Feed width	3
(a) Outer side	10.4	(Gw) Ground width	15
(b) Inner side	6.9		

The evolution stages of the MHLA antenna are depicted in Figure 2. As evidenced in Figure 3, the primary resonance for the hexagonal patch antenna occurred at nearly 3.35 GHz and the second harmonic resonance occurred at 5.4 GHz. To cover the lower band the hexagon patch was removed and the hexagon loop structure was used as a radiating patch. The resonance of the loop-based antenna shifted from 3.35 GHz to 2.85 GHz, whereas the second harmonic resonance of 5.4 GHz shifted to 6.4 GHz. It is well understood that both return loss and bandwidth cannot be enhanced simultaneously. This offered a 16.12% size reduction compared to the hexagon patch antenna. Further ground was tailored into curved shapes at both corners and it offered additional resonance near 4.2 GHz. Return loss decreased due to additional resonances.

Still, the return loss was well below -10 dB from the occurred resonance. A comparative return loss analysis and optimization is illustrated in Figure 3. It is evident from the return loss variation that the loop-based hexagonal patch with tailoring ground as curved ground plane provided better bandwidth.

(a) (b) (c)

Fig. 2. Evolution stages of the projected antenna: (a) MHPA with partial ground and CPW feed (ant 1), (b) MHLA with partial ground and CPW feed (ant 2), (c) MHLA with curved ground and CPW feed (ant 3).

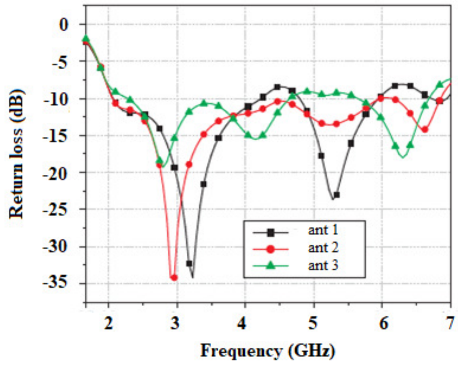

Fig. 3. Return loss variation for the evolution stages of the microstrip hexagonal antenna.

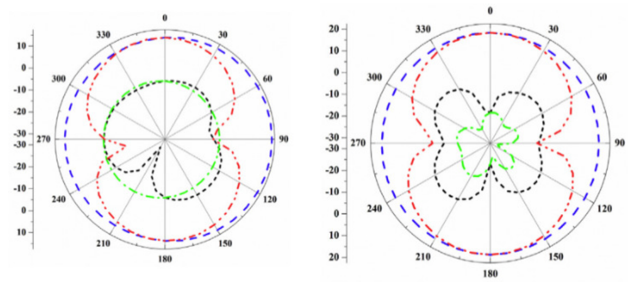

(a) (b)

Fig. 4. Radiation pattern at (a) 3.5 and (b) 5.8 GHz.

The radiation pattern was simulated for 3.5 GHz and 5.8 GHz, respectively, for co and cross-polarization. It is obvious from Figure 4 that a stable and bidirectional pattern was obtained for both the desired operation frequencies.

III. AMC DESIGN

The Artificial Magnetic Conductor (AMC) is a type of high-impedance surface and is most widely used to develop the radiation properties of different RF devices [14]. It offers high impedance at the resonance frequency of the designed unit cell. The resonance frequency and impedance equation are utilized as given in [13]. To increase the available inductance, the square loop's geometry was first developed as a square patch and then its shape was converted. Equations (1)-(3) from [13] were deployed to determine the resonance angular frequency of the AMC as well as the magnitude and phase of the AMC ground plane. When the denominator in (2) is 0, the surface has almost infinite impedance and functions as a perfect reflector.

$$\omega_0 = \frac{1}{\sqrt{LC}} \tag{1}$$

$$Z_{HIS} = \frac{j\omega L}{1-\omega^2 LC} \tag{2}$$

$$\theta = \mathrm{Img}\left[\ln\left(\frac{Z_{HIS}-n}{Z_{HIS}+n}\right)\right] \tag{3}$$

For a specific bandwidth, AMC exhibits in phase properties similar to those of PMCs (Perfect Magnetic Conductors) [14]. The 0^0-phase shift should occur at the resonance frequency (f_c), which in this case is 3.5 GHz. The bandwidth for the AMC is taken from -90^0 (lower frequency) to $+90^0$ (upper frequency). The effective wavelength (λ_{eff}) and the effective permittivity (ε_{reff}) values are calculated from the resonance frequency. Equation (4) is used to calculate the initial patch size *Lp:*

$$Lp = \frac{\lambda_{eff}}{2} \tag{4}$$

$$C = \frac{\varepsilon_{reff}}{2}\left(1 - 0.636\ln(koH)\right) \tag{5}$$

$$L = \mu_o H \tag{6}$$

where *L* and *C* stand for the overall inductance and capacitance that WB-AMC offers, respectively, and *H* stands for the substrate's thickness. The parameter is calculated utilizing rewritten versions of (4)-(6) from [11].

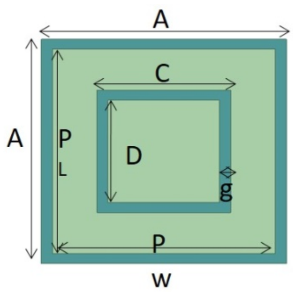

Fig. 5. The proposed AMC unit cell.

IV. PARAMETRIC ANALYSIS OF THE AMC MATRIX WITH THE PROPOSED ANTENNA

The gain of the designed antenna was nearly 4.2 dBi at 3.5 GHz and 2.6 dBi at 5.8 GHz without AMC integration. The proposed AMC unit cell as a [2×2], [3×3], and [4×4] matrix (Table II) was simulated with the designed hexagonal antenna with separation of 5 mm. The distance between the antenna and the AMC ground was selected at higher frequency to maintain minimum value. Figure 6 shows the different matrices of AMC unit cells. Return loss and gain variation are presented in Figure 7. The return loss and gain of the proposed antenna were degraded near 3.2 GHz and 5.8 GHz for [2×2] AMC ground plane, while better gain and return loss were obtained for [4×4] AMC ground.

TABLE II. AMC UNIT CELL DIMENSIONS

Parameters	Values (mm)	Parameters	Values (mm)
A	20	C	10
P_L	18	D	8
Pw	18	g	1

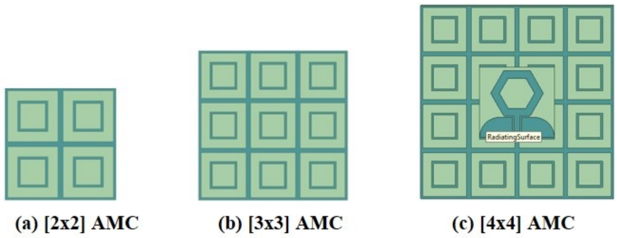

Fig. 6. Considered AMC cell matrices.

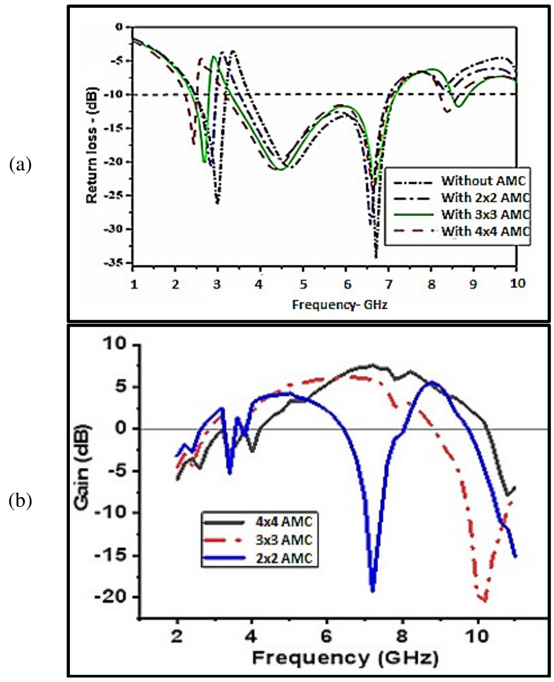

Fig. 7. (a) Return loss variation with AMC ground plane and the proposed antenna, (b) Gain variation with AMC of the proposed antenna.

V. RESULTS AND DISCUSSION

In this section, a thorough examination of the proposed high-gain MHLA antenna's performance in terms of gain, radiation pattern, and return loss variation is described. Figure 8 displays the stage 1 fabrication of a low profile, high gain MHLA antenna.

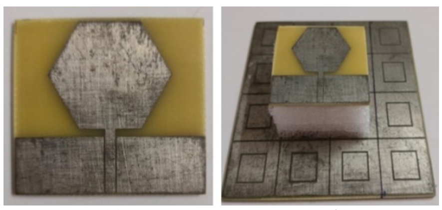

(a) (b)

Fig. 8. Fabricated low profile high gain MHLA antenna presented for stage 1.

A. Return Loss

Return loss is defined as the logarithmic value of the reflection coefficient (S11). The return loss was well below -10 dB between 2.6 GHz and 6.0 GHz for the proposed high gain MHLA antenna. Simulated and measured return loss comparison is observed in Figure 9.

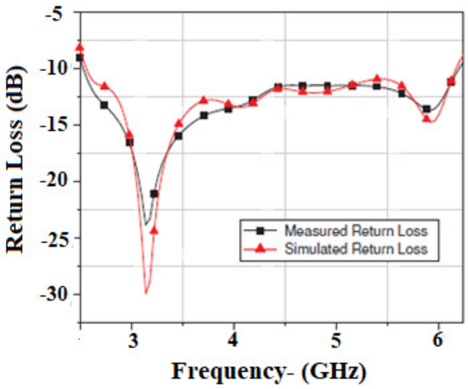

Fig. 9. Measured and simulated return loss of the proposed high gain MHLA.

B. Radiation Pattern, Gain, and Efficiency Analysis

Radiation pattern and gain analysis for the proposed antenna was carried out inside an anechoic chamber to avoid possible reflection during measurements. The simulation setup for the proposed antenna with AMC unit cell integration is manifested in Figure 10. The simulated and measured radiation patterns of the proposed high gain antenna in terms of Co and Cross polarization are presented in Figure 11. It is evident from the plot that more directive radiation pattern is obtained after the integration of the AMC ground plane. Figure 12 shows the measured gain and efficiency of the proposed antenna. Its efficiency is well above 70% between 2.5 GHz and 6.4 GHz. The gain achieved using AMC as ground plane is 5.3 dBi at 3.5 GHz and 8.2 dBi at 5.8 GHz, respectively.

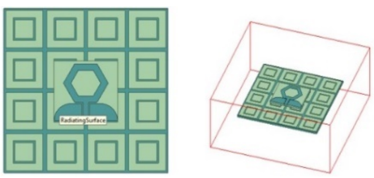

(a) (b)

Fig. 10. Simulation set up for radiation pattern and gain analysis.

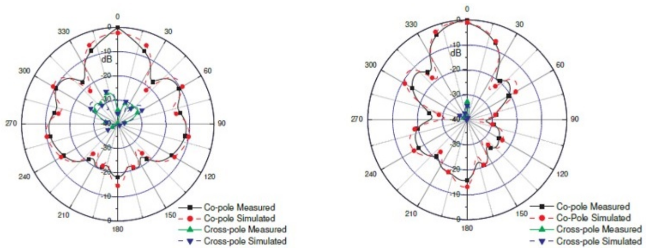

(a) (b)

Fig. 11. Measured and simulated radiation patterns of the proposed high gain MHLA at (a) 3.5 and (b) 5.8 GHz.

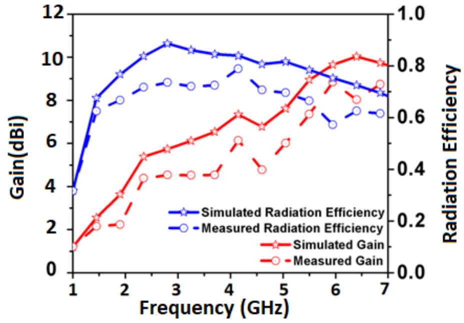

Fig. 12. Simulated and measured gain efficiency of the proposed high-gain MHLA antenna.

A comparison based on antenna size, bandwidth, gain, and structure complexity is presented in detail in Table III.

TABLE III. COMPARISON OF THE PROPOSED HIGH GAIN ANTENNA WITH REPORTED GAIN ENHANCEMENT WORK

Ref.	**Antenna size (*L×W*)**	**Ground size (mm)**	**Bandwidth (GHz)**	**Peak gain (dBi)**	**Cost analysis**	**Remarks**
[6]	40×40	60×61	1-2.8	~2.5	NG*	GAMA shape, fractal geometry
[8]	50×45	150×150	2-4.8	7.5	FR-4	FSS and slot
[7]	180×180	180×180	2.96-3.25	11.5	NG*	EBG and AIRGAP
[9]	90×80	110×100	1.6-6.7	9.9	NG*	DRA+ Reflector
Proposed	30×30	80×80	2.5 – 6.0	8.2	Economical (low-cost FR-4 substrate)	Square shape slotted AMC

NG*- datra not given

VI. CONCLUSION AND FUTURE WORK

In this paper, a high-gain MHLA was fabricated and tested for 5G and WLAN applications. Size reduction was obtained using a loop-based radiator and better return loss and bandwidth were acquired with the curved ground on either side of the CPW feed. The obtained return loss of the proposed antenna at 3.5 GHz was -22 dB without and -25 dB with the AMC ground plane. A peak gain of 8.2 dBi was achieved utilizing the AMC ground plane beneath the proposed antenna without disturbing the other antenna parameters. Experimental measurements were taken in an anechoic chamber and it was found that the measured and simulated results for return loss, gain, and radiation pattern were in good agreement with acceptable tolerance. Hence, the proposed MHLA high gain antenna is a good candidate for 5.8 GHz WLAN and 5G applications in the sub-6-GHz frequency range. The introduced wideband antenna can be designed for wearable technology in the future by employing flexible substrate material. Further, the distance between the antenna and the AMC can be minimized to make it more low-profile.

ACKNOWLEDGMENT

This work was funded by the University of Jeddah, Jeddah, Saudi Arabia, under grant No. (UJ-21-DR-122). The authors, therefore, acknowledge with thanks the University of Jeddah for technical and financial support. The author would like to acknowledge the experimental support provided by the VIT University Chennai campus, TN, India.

REFERENCES

[1] A. F. Vaquero, A. Rebollo, and M. Arrebola, "Additive manufacturing in compact high-gain wideband antennas operating in mm-wave frequencies," *Scientific Reports*, vol. 13, no. 1, Jul. 2023, Art. no. 10998, https://doi.org/10.1038/s41598-023-38247-x.

[2] M. Pons, E. Valenzuela, B. Rodriguez, J. A. Nolazco-Flores, and C. Del-Valle-Soto, "Utilization of 5G Technologies in IoT Applications: Current Limitations by Interference and Network Optimization Difficulties—A Review," *Sensors*, vol. 23, no. 8, Jan. 2023, Art. no. 3876, https://doi.org/10.3390/s23083876.

[3] R. P. Dwivedi and U. K. Kommuri, "CPW feed dual band and wideband antennas using crescent shape and T-shape stub for Wi-Fi and WiMAX application," *Microwave and Optical Technology Letters*, vol. 59, no. 10, pp. 2586–2591, 2017, https://doi.org/10.1002/mop.30786.

[4] K. R. Jha, N. Rana, and S. K. Sharma, "Design of Compact Antenna Array for MIMO Implementation Using Characteristic Mode Analysis for 5G NR and Wi-Fi 6 Applications," *IEEE Open Journal of Antennas and Propagation*, vol. 4, pp. 262–277, 2023, https://doi.org/10.1109/OJAP.2023.3249839.

[5] S. De and P. P. Sarkar, "A high gain ultra-wideband monopole antenna," *International Journal of Electronics and Communications*, vol. 69, no. 8, pp. 1113–1117, Aug. 2015, https://doi.org/10.1016/j.aeue.2015.04.012.

[6] K. Aliqab, S. Lavadiya, M. Alsharari, A. Armghan, M. G. Daher, and S. K. Patel, "Design and Fabrication of a Low-Cost, Multiband and High Gain Square Tooth-Enabled Metamaterial Superstrate Microstrip Patch Antenna," *Micromachines*, vol. 14, no. 1, Jan. 2023, Art. no. 163, https://doi.org/10.3390/mi14010163.

[7] L. Hardell and M. Carlberg, "Health risks from radiofrequency radiation, including 5G, should be assessed by experts with no conflicts of interest," *Oncology Letters*, vol. 20, Oct. 2020, Art. no. 15, https://doi.org/10.3892/ol.2020.11876.

[8] N. Kushwaha and R. Kumar, "Design of a wideband high gain antenna using FSS for circularly polarized applications," *AEU - International Journal of Electronics and Communications*, vol. 70, no. 9, pp. 1156–1163, Sep. 2016, https://doi.org/10.1016/j.aeue.2016.05.013.

[9] S. Agrawal, R. D. Gupta, M. S. Parihar, and P. N. Kondekar, "A wideband high gain dielectric resonator antenna for RF energy harvesting application," *International Journal of Electronics and Communications*, vol. 78, pp. 24–31, Aug. 2017, https://doi.org/10.1016/j.aeue.2017.05.018.

[10] C. R. Jetti and V. R. Nandanavanam, "Trident-shape strip loaded dual band-notched UWB MIMO antenna for portable device applications," *International Journal of Electronics and Communications*, vol. 83, pp. 11–21, Jan. 2018, https://doi.org/10.1016/j.aeue.2017.08.021.

[11] L. Peng, B.-J. Wen, X.-F. Li, X. Jiang, and S.-M. Li, "CPW Fed UWB Antenna by EBGs With Wide Rectangular Notched-Band," *IEEE Access*, vol. 4, pp. 9545–9552, 2016, https://doi.org/10.1109/ACCESS.2016.2646338.

[12] A. Suri and K. R. Jha, "Active frequency selective surfaces: a systematic review for sub-6 GHz band," *International Journal of Microwave and Wireless Technologies*, pp. 1–15, Nov. 2023, https://doi.org/10.1017/S1759078723001332.

[13] X.-J. Gao, T. Cai, and L. Zhu, "Enhancement of gain and directivity for microstrip antenna using negative permeability metamaterial," *International Journal of Electronics and Communications*, vol. 70, no. 7, pp. 880–885, Jul. 2016, https://doi.org/10.1016/j.aeue.2016.03.019.

[14] G. Gnanagurunathan and K. T. Selvan, "Artificial magnetic conductors on wideband patch antenna," *Progress In Electromagnetics Research Letters*, vol. 36, pp. 9–19, Jan. 2013.

[15] C. Joshi, A. C. Lepage, J. Sarrazin, and X. Begaud, "Enhanced Broadside Gain of an Ultrawideband Diamond Dipole Antenna Using a Hybrid Reflector," *IEEE Transactions on Antennas and Propagation*, vol. 64, no. 7, pp. 3269–3274, Jul. 2016, https://doi.org/10.1109/TAP.2016.2565695.

[16] N. K. Majji, V. N. Madhavareddy, G. Immadi, N. Ambati, and S. M. Aovuthu, "Analysis of a Compact Electrically Small Antenna with SRR for RFID Applications," *Engineering, Technology & Applied Science Research*, vol. 14, no. 1, pp. 12457–12463, Feb. 2024, https://doi.org/10.48084/etasr.6418.

[17] Y. E. Karasu, I. Uluer, and T. Ozturk, "An Investigation of the Effect of Embedded Gold Nanoparticles in Different Geometric Shapes on the Directivity of THz Photoconductive Antennas," *Engineering, Technology & Applied Science Research*, vol. 13, no. 4, pp. 11419–11425, Aug. 2023, https://doi.org/10.48084/etasr.6116.